File.

I.O.S.

INTERNAL DOCUMENT

90.

Preliminary Report of Medium Frequency Waves Measured on the Hebridean Shelf

J.M. VASSIE

Internal Document No 90

1980

NATURAL ENVIRONMENT RESEARCH COUNCIL

INSTITUTE OF OCEANOGRAPHIC SCIENCES

INSTITUTE OF OCEANOGRAPHIC SCIENCES

Wormley, Godalming,
Surrey, GU8 5UB.
(0428-79-2122)

(Director: Professor H. Charnock)

Bidston Observatory,
Birkenhead,
Merseyside, L43 7RA.
(051-652-2396)
(Assistant Director: Dr. D. E. Cartwright)

Crossway,
Taunton,
Somerset, TA1 2DW.
(0823-86211)
(Assistant Director: M.J. Tucker)

Marine Scientific Equipment Service
Research Vessel Base,
No. 1 Dock,
Barry,
South Glamorgan, CF6 6UZ.
(04462-77451)
(Officer-in-Charge: Dr. L.M. Skinner)

Preliminary Report of Medium Frequency Waves Measured on the Hebridean Shelf

J.M. VASSIE

Internal Document No 90

1980

This Project was funded by the Department of Energy

ABSTRACT

This document is intended as a preliminary report on the Medium Frequency Wave Project carried out during November and December 1979. During these months a recorder was deployed west of the Hebrides to measure waves in the frequency range 0.1mHz (3 hour period approximately) to 30mHz (33 second period). A total of 27 days of data was obtained, during which waves were recorded for 3 hours on each day at 3 second intervals.

The report describes the experiment and some of the data obtained. Up to this point in time not all the data have been analysed, but a few selected records are presented with their corresponding power spectra corrected for depth attenuation. These have been chosen purposely to represent periods when the wind wave amplitude was minimal, was of medium intensity and was the most extreme during the recording period.

The root mean square amplitude of medium frequency (m.f.) wave is derived and shown to depend approximately on the square of the r.m.s. amplitude of the wind waves, suggesting that the low frequency variations are driven by the Bernoulli effect ($\frac{1}{2}\rho u^2$ where u is the current velocity associated with the wind wave amplitude). This is reinforced by cross-correlation functions of the m.f. waves and the wind wave envelope which show these two to be negatively correlated instantaneously. This would correspond to radiation stresses in the wave groups causing a depression in the mean surface level (Longuet-Higgins & Stewart 1962). The absence of a significant component at the second harmonic of the wind wave peak suggests that the effect is not due to dynamic pressures on the recorder itself.

Prediction of the m.f. waves from the wind wave envelope accounts for 50% of the observed variance. However, this value is

low for reasons given in the report. It is expected the m.f. variations will be almost completely explained by non-linear effects in the wind waves leaving only a small amount of residual m.f. energy.

It should be mentioned that these latter results are obtained from only four of the available 27 wave records. When the remainder are analysed they may reinforce or modify the results. However, the spectra have been computed for nearly one-third of the records and m.f. wave variance has been computed for all the available records and these show characteristics in agreement with the four examples quoted in this paper.

1. Introduction

Medium frequency waves occupy a valley in the spectrum between the lower frequency tides and the high frequency wind waves, both of which are energetic and have been the subject of intensive study. A range of instrumentation has been developed to measure tides and wind waves, but the frequency response of both sets of instruments is designed specifically to cut-off in the m.f. range in order to eliminate the other part of the spectrum. Equipment designed to measure waves in the m.f. region has been built (e.g. Munk, Snodgrass & Tucker 1959) but is not available commercially.

Lately however a knowledge of the energy density in the m.f. region has become important because large offshore structures such as semi-submersible drilling platforms and wave energy devices have resonant periods of a few minutes which make them susceptible to m.f.waves. The initial requirement is to evaluate orders of magnitude to see if the effects of the waves on the structures are significant. Considerable research on such waves has been carried out in the U.S.A. (e.g. Munk 1962) but little is known about their characteristics on the U.K. continental shelf. A summary of what is known has been prepared recently by Huthnance (1979).

To obtain this information and to identify sources of medium frequency energy, a pressure recorder was deployed on the sea bed at position 57^{o} 18' 15''N, 07^{o} 39' 30''W, which is 17km west of the Hebrides, in 50 metres of water (figure 1). Northern Scotland is well known for the presence of oscillatory periods of several minutes on tide gauge records and the site was chosen to be in an area of strategic importance for wave energy conversion. The medium frequency recorder was placed in a sandy hollow, where the topography was reasonably flat, to reduce any non-linear bottom effects induced by the currents. Inshore however the sea bed was

quite rough and this was the reason the instrument was deployed 10m deeper than was originally intended. It was proposed to install a surface wave recorder above the m.f. recorder but this was not possible due to extremely adverse weather conditions. However a waverider belonging to the Institute of Oceanographic Sciences (IOS) was in operation some 10 miles distant which should provide some comparisons of the measured wind waves.

The m.f. recorder is a modified offshore tidal pressure recorder designed by IOS for deep ocean measurements. In normal operation the output from a frequency modulated pressure sensor is integrated by a digital counter over 15 minutes and logged on magnetic tape, and the counter reset to zero. Each count is then a measure of the average bottom pressure during the previous 15 minutes which is the combined effect of atmospheric pressure, hydrostatic pressure and pressure due to surface elevation movements. The waves are attenuated by the integrating process of the instrument.

The electronics in the recorder were modified to sample the integrated count from the pressure sensor every 3 seconds without re-setting the counter for a period of 3 hours each day. For the remaining 21 hours the instrument operated in the normal tide recording mode. During the wave periods the pressures are the combined effect of atmospheric pressure, tidal height and waves limited by depth attenuation to an upper frequency of approximately 167mHz, a period of 6 seconds.

The sampling rate of 3 seconds for a period of 3 hours was governed principally by the digital capacity of the cassette tape in the data logger. This choice was a compromise between recording the high frequency waves without much aliasing and obtaining a reasonably long daily sample with adequate resolution for the m.f.

waves and yet obtaining a fair seasonal sample of the wave climate.

The deployment should have lasted 35 days but ended prematurely when the acoustic release fired on the noise generated by a severe storm. Fortunately, the recorder was cast up on a nearby beach from which it was recovered undamaged. It was later found to contain 27 days of recorded waves and tides.

2. The Data

The raw data from the instrument is essentially a measure of the frequency output from the pressure sensor and requires conversion to pressure by calibrations which are carried out before and after deployment. For convenience the pressure 'p' is quoted in millibars (mbar) because this is almost identical to centimetres of surface elevation ζ . The exact relation for the surface pressure is $p_s = \rho g \zeta$ where ρ is the density of sea water and g is the gravitational acceleration. For the deployment site ρg is taken as 1.0051 mbar/cm.

At the bottom the pressure is attenuated with wavelength and the relation is given by equation 1.

$$p_b = \rho g \zeta \operatorname{sech}(kd) \quad \text{——} \quad (1)$$

$2\pi/k$ = wavelength

d = depth

The attenuation is important for high frequency waves and is only negligible for medium and low frequency ranges.

The tidal record can be considered separately from the wave records of which there are 27 each spanning 3 hours. The tidal record contains fluctuations with frequencies ranging between 0 and 0.6mHz which overlaps somewhat with the wave spectra and can be used to estimate power densities of waves near the tidal frequencies. The wave records contain pressure fluctuations primarily between 0.1 mHz and 167 mHz. High frequency waves in general occupy frequencies greater than this which are therefore aliased but not too seriously because of the attenuation with depth.

The instrument responds to all frequencies below 167mHz and therefore the wave records are superimposed on a tidal profile which has to be removed to make the wave records useful. The range of tide west of the Hebrides is approximately 4m at springs which, compared to m.f. waves of a few centimetres, is too large to be removed by a traditional synthesis of tide from known harmonic constants. Neither was it thought appropriate to remove the tide by high pass filtering because of the inherent loss of data at the beginning and end of the records. Instead the tidal profile was fitted by a cosine tapered Fourier series whose coefficients were used to predict the tidal component of each 3 sec wave observation.

The equations are given below. The coefficients a_o , a_j , b_j , $j = 1(1)8$ are the pairs of coefficients of the fourier harmonics between 1 cycle/day and 8 cycles/day, and x_k is the 15 minute pressure at time k centred on k = 48. The term C_k is a cosine taper used to reduce end effects.

$$C_k = 1 + \cos k\pi/48$$

$$p_{jk} = C_k \cos jk\pi/48 \qquad k = 1(1)47$$

$$q_{jk} = C_k \sin jk\pi/48 \qquad j = 1(1)8$$

$$a_o = \frac{1}{96}\left[2\,x_{48} + \sum_{k=1}^{47} C_k(\,x_{48+k} + x_{48-k})\right]$$

$$a_j = \frac{1}{48}\left[2\,x_{48} + \sum_{k=1}^{47} p_{jk}(\,x_{48+k} + x_{48-k})\right]$$

$$b_j = \frac{1}{48}\sum_{k=1}^{47} q_{jk}(\,x_{48+k} - x_{48-k})$$

If $t_{m,n}$ is the time of the n'.th wave scan following tidal scan m then

$$t_{m,n} = m - 47.5 + (n-0.5)/300 \qquad \begin{matrix} m = 42(1)53 \\ n = 2(1)300 \end{matrix}$$

and the high passed wave series $w'_{m,n}$ is obtained from the recorded waves $w_{m,n}$ as

$$w'_{m,n} = w_{m,n} - (1 + \cos\tfrac{\pi}{48}t_{m,n})^{-1}\left[a_o + \sum_j (a_j \cos\tfrac{\pi}{48}jt_{m,n} + b_j \sin\tfrac{\pi}{48}jt_{m,n})\right]$$

The Fourier series was fitted to the 15 minute tidal series over a period of 24 hours such that each wave block was situated in approximately the centre of the 24 hours. Removal of the tidal component in this manner effectively eliminates variations of period longer than 3 hours and passes those whose period is less than 2.4 hours without attenuatuon of amplitude.

The effectiveness of this technique can be judged from the spectrum shown in figure 6 for the high passed tidal series where the variance of the species 2 tide at 0.02mHz is 4 orders of magnitude below the m.f. level.

Some examples of the high passed wave records are shown in the upper frames of figure 2. a) through d). Figure 2c correspond to a quiet period and figure 2d to the time when the wind waves were the most energetic during the deployment. The size of the waves during the period is indicated in Table 1 by the total variance of the records measured at the sea bed.

TABLE 1

Record Number	Date	Wind Speed (knots)	Wind Direction (degrees)	Total variance at sea bed $(mbar)^2$
2	21/11/79	16	210	709.8
13	2/12/79	24	240	4226.8
19	8/12/79	10	90	76.9
24	13/12/79	30	210	6944.9

The records have the appearance of groups of waves propagating through the area. The length of the groups is some 15 times the wind wave period and can be considered long compared to the depth. Obviously the surface elevation giving rise to these pressure fluctuations on the bottom is somewhat different because the waves are more attenuated as their frequency increases. The bottom pressure records therefore lack some of the high frequency content of the surface. Nevertheless one would expect the surface to maintain the appearance of wave groups.

The weather conditions during the deployment period were quite severe but they did vary considerably from day to day and waves of varying amplitudes were recorded. The smallest were during record 19 when the significant wave height (H_s) was little more than 70 cm at the surface, the largest was record 24 when H_s was near 700 cm. The statistics of the surface cannot of course be deduced directly from the pressure records because the depth attenuation is frequency dependent but they can be found from the spectrum of the wave records.

3. Spectra of Wave Records

The power density spectra have been computed for about one-third of the available wave records using the Fast Fourier Transform. Each 3 hour record of 3600 samples is split into 7 pieces of length 512 and the spectral analysis performed on each piece. To each piece a 10% cosine taper is applied to improve the shape of the spectral window and thereby reduce the leakage of energy from the wind wave frequencies into the m.f. region.

The spectrum of each piece has a resolution of 0.6m Hz in 256 bands from 0.6m Hz to 167m Hz. The harmonics are averaged in pairs and finally the 7 pieces are averaged to produce a wave spectrum for each 3 hour record, the resolution of which is 1.3mHz. This procedure guarantees that the leakage into the m.f. range is well below 10^{-6} of the wind wave power. The spectra for the 4 records previously discussed are shown in figure 3.

All the spectra so far computed show the same characteristic shape. The m.f. region is reasonably flat up to 20mHz above which there is a valley before the rapid rise of the wind wave region which is typically 3 orders of magnitude greater than the level of the m.f. waves. The m.f. level in the spectra rises when there is an increase in the wave activity. The maximum level reached was 1.8 $mbar^2/mHz$ which is equivalent to a total variance of 36 $mbar^2$ in the region up to 20mHz.

The peak in the wind wave spectra is followed by an almost exponential decrease in power with increasing frequency, depth attenuation being the most important component of this. The position of the peak varies with the mean wind speed and

migrates to lower frequencies as this rises. Its position is denoted by the peak period, Tp and can be related to the mean zero of cross-period T_z (Goda 1974). Some values of Tp derived from the present data are included in Table 2. These values are unaffected by depth attenuation.

It has been suggested that the lack of a second spectral peak above the main peak is indicative that the m.f. energy is not simply a non linear Bernoulli effect on the instrument. One could expect that currents induced by the waves might produce a pressure of $\frac{1}{2}\rho u^2$ on the instrument. However, if this were so, a second harmonic of the main peak would be expected with energy levels comparable with the low frequency components. Because the second harmonic is absent it can be concluded that the m.f. energy is real and not instrumental.

The attenuation of the high frequency waves in 50m of water is quite severe. Typically a wavelength of twice the depth (f = 125mHz) is attenuated to 1% of its surface value. Correction of the spectra for attenuation has been done using Equation 2. (See for example Pierson and Marks 1962).

$$P_s(f) = P_b(f) . \cosh^2(k.d) \qquad (2)$$

where P_s is the surface pressure spectrum

P_b is the bottom pressure spectrum

d = depth in metres

k = wave number calculated from the angular frequency w by the dispersion relation

$w^2 = gk \tanh(kd)$

If desired the surface elevation spectrum may be calculated from $P_s / (\rho g)^2$. The correction equation has negligible effect for the m.f. waves but at the nyquist frequency the correction is

of the order of 10^5 making the spectrum unreliable at very high frequencies.

The high frequencies are also attenuated by the integration of the signal from the pressure transducer proportional to $\sin(\pi fT)/\pi fT$ where T = 3 sec. This correction is generally small compared to the depth attenuation but in energy terms reaches 2.5 near the nyquist frequency: here, however, it is approximately cancelled by the folding back of energy above the nyquist frequency.

The corrected spectra are superimposed on the uncorrected spectra in figure 3. They have been compared with the Pierson-Moskowitz (PM) spectra for fully developed seas (Pierson & Moskowitz 1964) and are similar in shape except for the rise in energy at high frequencies. The main difference at lower frequencies is the frequency of the spectral peak in relation to its height. The measured spectra appear to have their peak at a higher frequency than the PM spectra which would be the case if the seas were not fully developed.

The rise in spectral energy above 120mHz is not fully understood and is being examined at the present time. It is present in the uncorrected spectra as a departure from the exponential decrease in energy with frequency. Partly it is due to aliased power which is not totally eliminated by signal integration and of course the depth correction terms are large at high frequencies but this does not explain it completely.

Surface measurements made by the Institute of Oceanographic Sciences (Taunton) in the same area which are to be published shortly by Ewing (IOS Wormley) indicate that the spectra fall off more slowly than the generally accepted law of $P(f) \propto f^{-5}$.

However, they do not show the increase in power found here. The two possibilities being examined are whether the energy is generated at beat frequencies of the main wind waves in much the same manner as the m.f. waves are generated at the difference frequencies or whether they are the result of standing waves (Longuet-Higgins 1973). In the former case the process would have to occur at depth making the depth correction terms inappropriate otherwise the effect would be evident in surface spectra. In the latter case the depth correction is again inappropriate. A third possibility is that the complicated topography surrounding the area is in some way the cause.

From the corrected spectra (P(f)) the significant wave height (H_s) at the surface may be estimated as $H_s = 4\sigma$ where

$$\sigma^2 = \frac{1}{(\rho g)^2} \int_{f_{min}}^{\infty} P(f).df \qquad (3)$$

f_{min} = lower limit of wind waves

The values of H_s and the peak period, Tp, are shown below. Obviously the values are limited by the fact that the spectra do not extend to the upper limits of the wind wave frequencies but because the bulk of the energy is contained near the spectral peak they should be correct to a first order. Record 15 is anomalous in that its Tp is low for the derived value of significant wave height. It has been found to be anomalous in other respects.

TABLE 2

Record Number	Peak period T_p (sec)	Significant Wave Height H_s (cm)
19	10.8	70.7
7	11.3	128.3
2	13.7	216.5
9	13.5	226.3
23	15.1	247.0
21	14.8	318.6
14	15.4	404.9
15	13.2	442.0
13	16.0	527.8
24	17.9	674.2

In the 4 spectra shown in figure 3 the m.f. level obviously bears some relationship to the level of the wind waves but this is more obvious by splitting the records w(t) into time series m(t) and z(t) corresponding to the m.f. and wind wave spectral regions.

4. Filtered records

The two time series m(t) and z(t) were separated from the observed records by a low pass filter with a half amplitude point at 30mHz. Its characteristic is close to unity for frequencies below 18mHz and close to zero for frequencies above 42mHz. The filter causes the loss of 19 terms at the beginning and end of the record but this is not considered serious. The time series m(t) is realistic in the sense that it is representative of surface conditions. It is impossible however to recreate the surface wind wave record exactly because the attenuation is frequency dependent.

The m.f. waves from the filter are included in figure 2 for comparison with the profile of the recorded waves. The surface movements associated with the m.f. region are apparently several tens of centimetres. The equivalent of significant wave height estimated from the variance of m(t) is tabulated below.

TABLE 3

Record Number	Significant Wave height of m(t) (cm)
18	2.3
5	3.0
4	3.1
7	3.1
1	3.1
19	3.2
6	3.8
8	4.0
17	4.1
22	4.1
10	4.4
3	4.6
11	4.6
26	4.9
2	4.9
20	4.9
9	5.2
16	5.9

TABLE 3 (cont.)

Record Number	Significant Wave height of m(t) (cm)
23	6.0
12	6.0
27	7.4
21	7.9
25	8.6
14	11.3
13	16.8
15	17.0
24	24.7

The most obvious result from figure 2 is the reduction in the level of m(t) coincident with a high wave group. There are numerous occasions when set-down occurs with a duration similar to that of the wave groups.

A strong relationship is found if the root mean square (r.m.s.) of the m.f. series is plotted against the r.m.s. value of its assocated wind wave record. This has been done for the 27 wave records and the results are shown in figure 4. The relationship is non-linear and in fact indicates that m(t) increases as the square of z(t) suggesting that m(t) is caused by radiation stresses under the waves (Longuet-Higgins & Stewart 1962). Conditions here are similar to those discussed by these authors where the lengths of the groups are large compared to the depth.

Another important fact is that the curve approaches the origin for low wave amplitudes inferring that there is little or no background m.f. motion. Certainly the background level is below 0.06 mbr^2/mHz which was recorded during the quietest period.

5. Relation between m.f. waves and wind wave envelope

Cross correlation of m(t) with the wind wave envelope y(t)

serves to illustrate the time dependence of the two series. The wave envelope is defined here by equation 4 as the mean square of the wind wave record

$$y(t) = \frac{1}{2T_z} \sum_{s=-T_z}^{T_z} z^2(t+s) \qquad (4)$$

over two zero crossing periods. The mean square is used in preference to any other function because the relationship based on the evidence of figure 4 is expected to be second order.

Figure 5 contains the cross correlation $\phi(\tau)$ as a function of lag τ between the two variables m(t) and y(t). The curve is not plotted for record 19.

$$\phi(\tau) = \frac{\sum m(t).y(t+\tau)}{\left[\sum m^2(t) . \sum y^2(t)\right]^{\frac{1}{2}}} \qquad (5)$$

$$\sum \equiv \sum_{t=1}^{N}$$

because the variations are minimal during this period.

The other records show a high negative correlation of about -0.6 at zero lag indicating set-down beneath the wave groups. The major part of the m.f. variations is therefore locally generated and is almost certainly due to radiation stresses in the waves. It is possible the zero-lag correlation is higher than 0.6 as is discussed in the following paragraph on the response function.

The correlation at non-zero lags is low, especially for negative lags i.e. m.f. waves preceding wind waves. There is however a correlation of 0.2 at a positive lag of 750 sec for

both record 13 and 24 which were the largest recorded. The time delay is short for this to be caused by long waves propagating from the surf zone which is 17 km from the deployment site. Tucker (1950) found a high negative correlation between wind waves and m.f. waves separated by the time taken for the wave groups moving at the group velocity to reach the surf zone and for the free waves to propagate to the recorder site. Here, with a group velocity of 15 m/s and a free wave velocity of 16 m/s the minimum time delay is of the order of 36 minutes. Small values of correlation of the correct sign do appear at lags between 40 minutes and 45 minutes. These are not included in figure 5 because their magnitude of -0.1 is only just above the noise level in the correlation function and consequently their contribution to the m.f. variance is minimal in comparison to the instantaneous effect of set-down.

At positive lags the correlation function is slightly periodic. It may be that the wave groups lose energy as they move inshore and that they result in free waves propagating seawards which produce the positive and negative correlations depending on the phase of the free wave when it reaches the recorder.

Prediction of the m.f. variations in the time domain is possible from the associated high frequency series. Figure 7 shows an example for 1 hour of the medium frequency record from block 13 which is the only data so far used.

The response function between the wind wave envelope and the m.f. waves has been calculated as a series of response weights of different lags as in equation 6.

$$m_1(t) = \bar{y} + \sum_n a(n).y(t - n\Delta\tilde{\tau}) \qquad (6)$$

where $m_1(t)$ = predicted m.f. variations

$y(t)$ = wind wave envelope as in equation 4.

$a(n)$ = response weights $n = -N(1)N$.

$\Delta\tilde{\tau}$ = lag between response weights = 27 seconds

$\bar{y}$ = mean level of $y(t)$

The response weights are derived by minimising the mean square error between $m_1(t)$ and $m(t)$ (See for example Robinson & Silvia 1978). Strictly the procedure is applicable to linear systems only but generating the wind wave envelope as in equation 4 produces near linearity.

In practice the only significant response weight is found to be the one at zero lag, the others contribute a negligible amount to the m.f. variations as one might expect from the shape of the correlation function. The example shown in figure 7 indicates that the predicted variations agree reasonably well with those observed, especially during periods of severe set-down. For this particular case the predictable variance is about 50% of that observed which again is in agreement with the correlation coefficient of -0.6. However, it is somewhat less than expected.

Using equation 7 to estimate the currents $u(t)$ associated with the wind waves (see for example Cartwright 1962) the

$$u(t) = \frac{p(t)}{\rho g}\omega.\coth(kd) \qquad (7)$$

Bernoulli effect giving rise to the low frequency variations (equation 8) can be estimated. This appears to account

$$p = \tfrac{1}{2}\rho u^2 \qquad (8)$$

for much more than 50% of the variance for particular wave groups but the exact figure for the whole record has not been calculated. Close examination of figure 7 reveals that the residual variance is confined to the high frequency components of the m.f. range. It is probable that the deficiency in predicting the m.f. variations is due to a lack of high frequency components in the wind wave envelope because of the manner in which it is generated (equation 4). However, there is a difficulty in producing the high frequency components because their frequency is close to that of the wind waves themselves. When the difficulty is overcome the m.f. variations may well be attributable to non-linear processes in the waves with very little contributed from other sources.

6. High Frequency Tidal Spectrum

The high frequency tidal series was generated in the same manner as the wave series by removing a tapered Fourier series fitted to the tidal data. It is included here mainly for completeness since the frequency range covered is also covered by the wave series. The spectrum shown in figure 6 represents the mean power density over the 27 day period. The level of 0.5 mbar /mHz at high frequencies is low by a factor of 2.5 due to instrument attenuation but some aliasing is probable from waves above the nyquist frequency. The aliased power could be evaluated from the wind spectra but this has not been done.

Summary

The work carried out so far indicates that medium frequency waves in the area can be several tens of centimetres. The largest recorded during the deployment had a significant wave height of 25 cm. Power spectral density in the m.f. range 0.1 mHz to 30 mHz reached a maximum of 1.8 $mbar^2/mHz$.

The spectra, corrected for depth attenuation, show the m.f. region to be reasonably flat to a frequency of 20 mHz. Above this the power density falls until at 40 mHz there is a sharp rise into the wind wave region. The wind wave region shows characteristics similar to the Pierson-Moskowitz spectra but are more in agreement if the seas are assumed to be not fully-developed. The rise in spectral power above 120 mHz is not fully understood and is being examined.

Comparing the r.m.s. amplitude of the m.f. variations with that of the associated wind waves suggests that the relationship is second order which is in agreement with radiation stresses inducing set-down of the surface. No background m.f. energy is evident under conditions of low wind speeds.

The major part of the m.f. variations are almost certainly caused by set-down under the wave groups. This has been shown by the dominance of the zero lag coefficient in the correlogram and by the importance of the zero lag term in the response function. The correlation function shows some evidence of free waves propagating from the surf zone but their contribution to the total variance is small.

Estimating the predictable amount of m.f. variance from the wind wave envelope gives 50% but this is thought to be an

underestimate because of the manner in which the envelope was generated. Simple calculations based on the Bernoulli effect suggest that the predictable variance should be much higher.

References

Cartwright, D.E. 1962. Chapter 15 in 'The Sea', Vol 1. ed. M.N. Hill, Wiley, London pp 567-588.

Ewing, J. Observations of Wind Waves and Swell at an Exposed Coastal Location. Estuarine and Coastal Marine Science (In Press).

Goda, Y. 1974. Estimation of Wave Statistics from Spectral Analysis Information. Proc. International Symp. on Ocean Waves, Measurement and Analysis.

Huthnance, J.M., 1979. An Outline Review of Medium Frequency Waves. Institute of Oceanographic Sciences Report No. 81. (Unpublished Manuscript).

Munk, W.H. 1962. Long Ocean Waves. Ch. 18 in The Sea Vol. 1, ed. M.N. Hill, Wiley, London, 864 pp.

Munk, W.H., Snodgrass, F.E., and Tucker, M.J. 1959. Spectra of Low frequency Ocean Waves. Bull, Scrips. Inst. Oceanogr., 7, 283-362.

Pierson, W.J. & Marks, W. 1962. The Power Spectrum Analysis of Ocean Wave Records. Trans. Amer. Geophys. Union, Vol. 33 No. 6 Dec.

Longuet-Higgins, H.S. & Stewart, W.R. 1962. Radiation Stress and Mass Transport in Gravity Waves with Application to 'Surf Beats'. Jour Fluid Mech. Vol. 13 Pt 4 pp 481-504.

Longuet-Higgins, H.S. 1973. On the Form of the Highest Progressive and Standing Waves in Deep Water. Proc. R. Soc. Lond. A331, 445-456.

Tucker, M.J. 1950. Surf Beats: Sea Waves of 1 to 5 Minutes Period. Proc. Roy. Soc. A, 202, 565-73.

Pierson, W.J. & Moskowitz, L. 1964. A Proposed Spectral Form for Fully Developed Wind Seas Based on the similarity Theory of S.A. Kitaigorodskii. J. Geophys. Res. 69, 5181.

Robinson, E.A. and Silvia, M.T. 1978. Digital Signal Processing and Time Series Analysis. Holden-Day Inc., San Francisco pp 89-98.

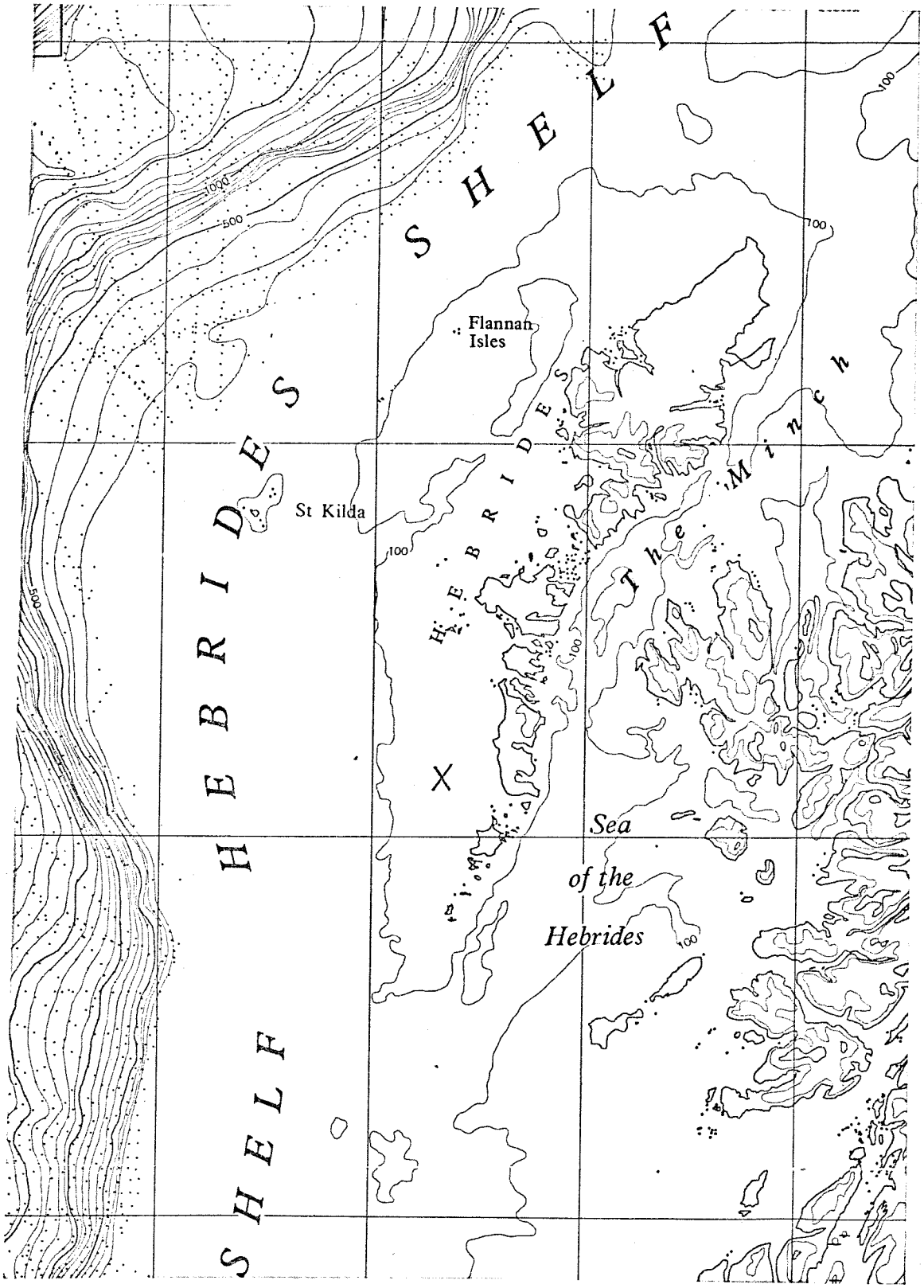

FIGURE 1 : MAP OF THE DEPLOYMENT AREA.
LOCATION OF M.F. RECORDER SHOWN BY X.

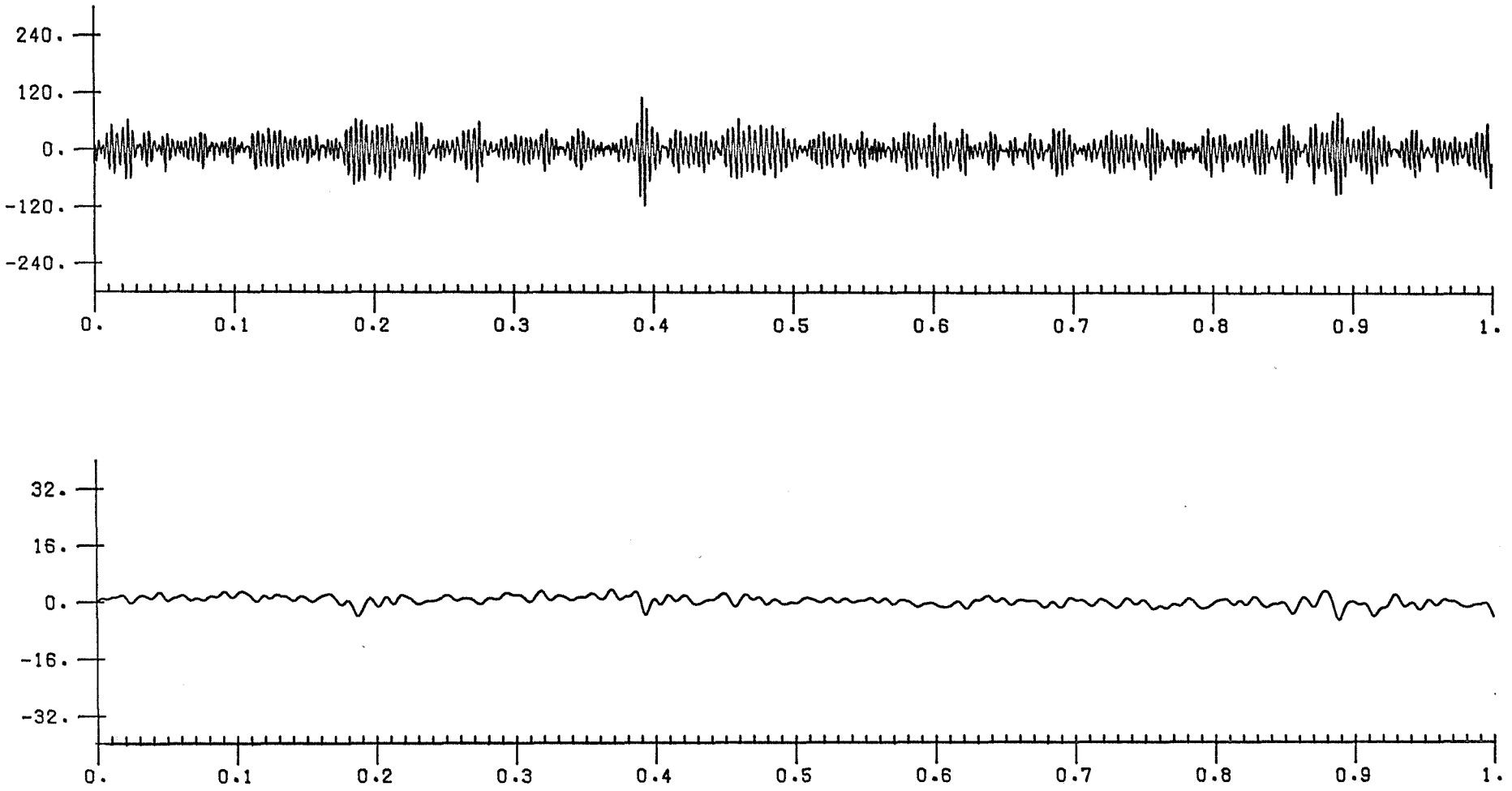

FIGURE 2A : WAVE RECORD 2 21/11/79.

THE UPPER FRAME SHOWS THE RECORDED WAVE PRESSURES AT THE SEA-BED WITH THE TIDES REMOVED.

THE LOWER FRAME SHOWS M.F. WAVES DERIVED BY LOW PASS FILTERING THE RECORDED WAVES.

PRESSURES ARE IN MBARS
HORIZONTAL AXIS IN HOURS.

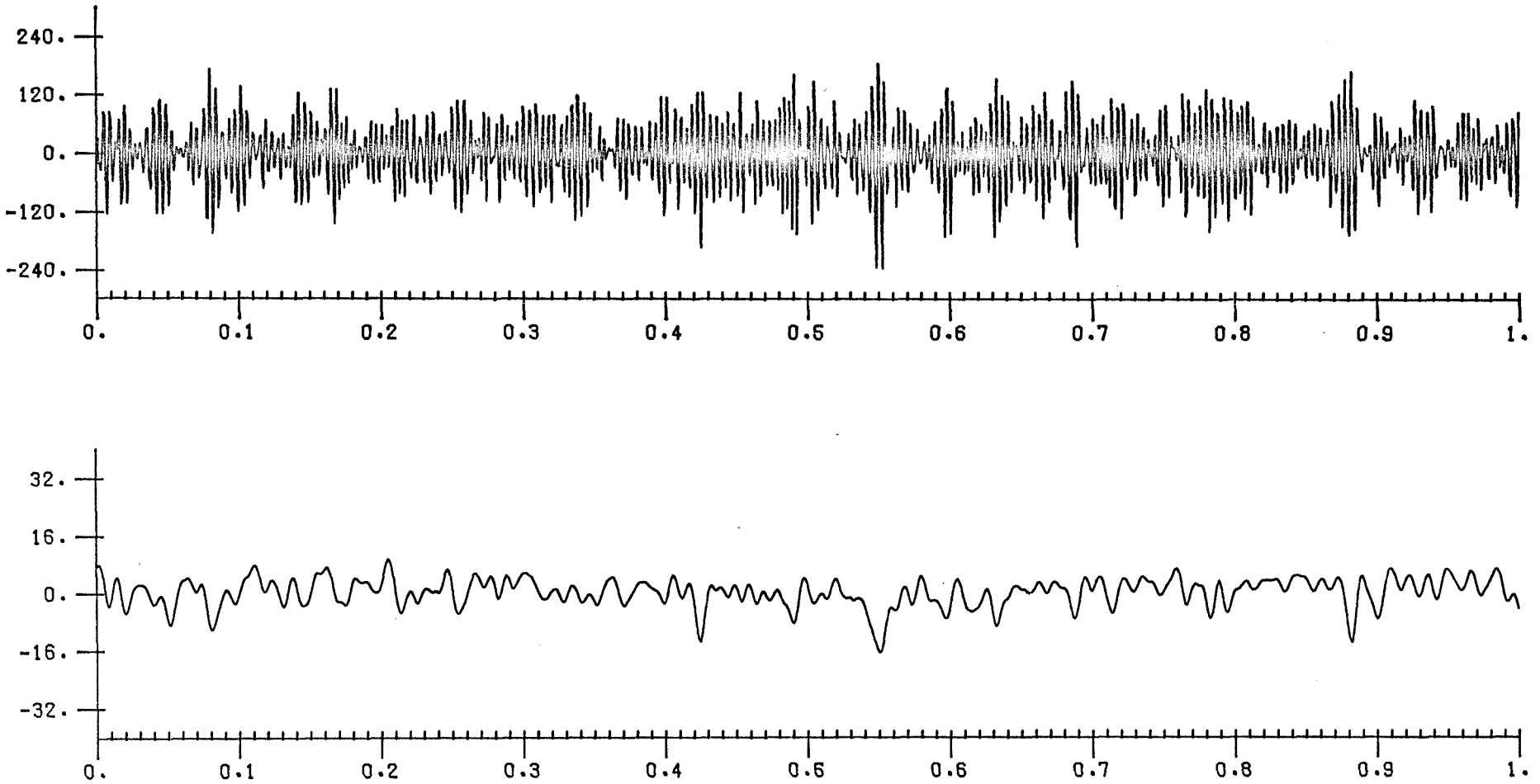

FIGURE 2B : WAVE RECORD 13 2/12/79.

THE UPPER FRAME SHOWS THE RECORDED WAVE PRESSURES AT THE SEA-BED WITH THE TIDES REMOVED.

THE LOWER FRAME SHOWS M.F. WAVES DERIVED BY LOW PASS FILTERING THE RECORDED WAVES.

PRESSURES ARE IN MBARS
HORIZONTAL AXIS IN HOURS.

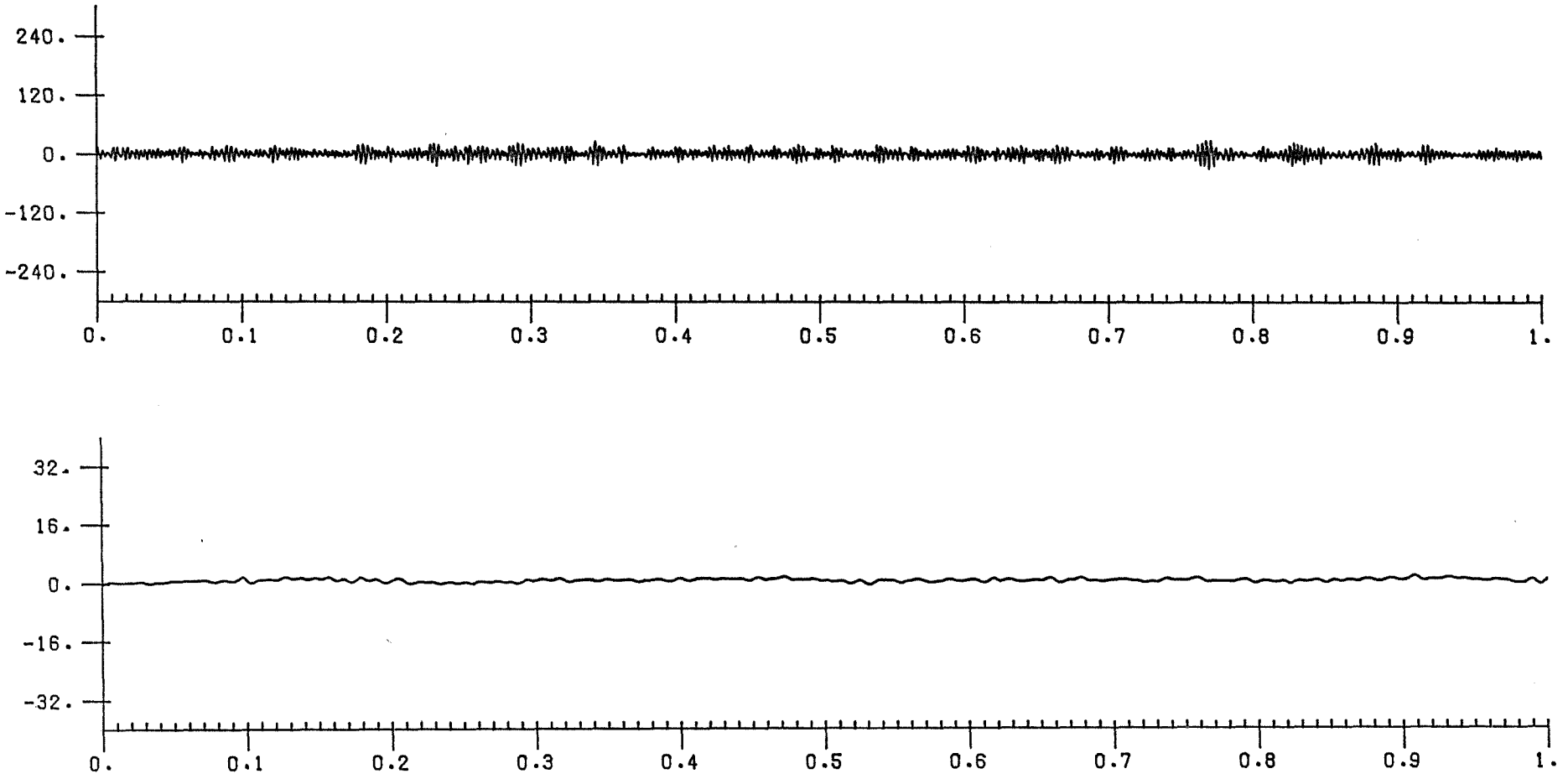

FIGURE 2C : WAVE RECORD 19 8/12/79.

THE UPPER FRAME SHOWS THE RECORDED WAVE PRESSURES AT THE SEA-BED WITH THE TIDES REMOVED.

THE LOWER FRAME SHOWS M.F. WAVES DERIVED BY LOW PASS FILTERING THE RECORDED WAVES.

PRESSURES ARE IN MBARS
HORIZONTAL AXIS IN HOURS.

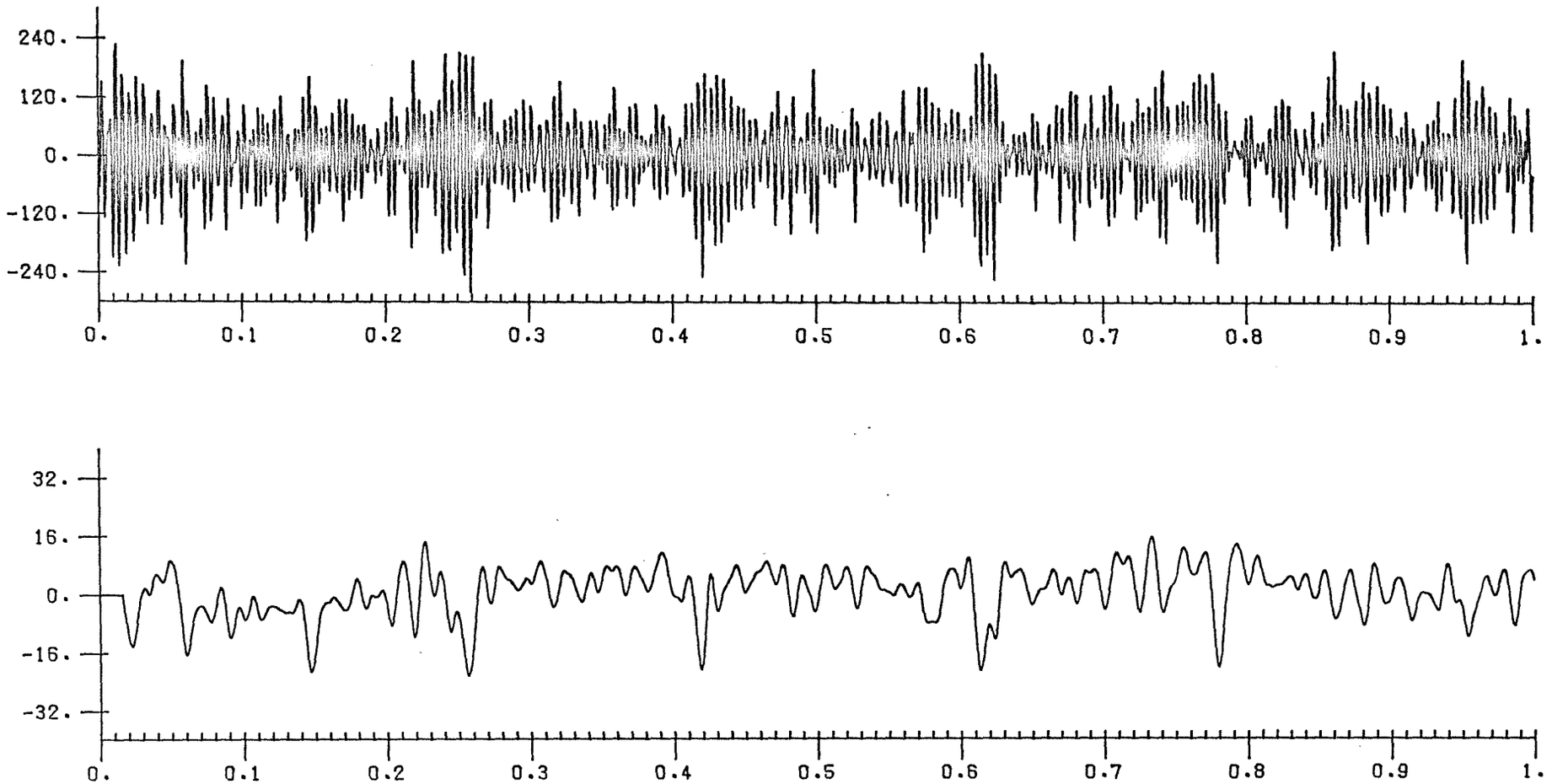

FIGURE 2D : WAVE RECORD 24 13/12/79.

THE UPPER FRAME SHOWS THE RECORDED WAVE PRESSURES AT THE SEA-BED WITH THE TIDES REMOVED.

THE LOWER FRAME SHOWS M.F. WAVES DERIVED BY LOW PASS FILTERING THE RECORDED WAVES.

PRESSURES ARE IN MBARS
HORIZONTAL AXIS IN HOURS.

FIGURE 3A : POWER DENSITY SPECTRUM OF RECORD 2.

THE LOWER GRAPH IS THE SPECTRUM OF MEASURED SEA-BED PRESSURES.

THE UPPER GRAPH IS THE SPECTRUM CORRECTED FOR DEPTH ATTENUATION.

P(f) IN MBAR^2/mHz. f in m Hz.

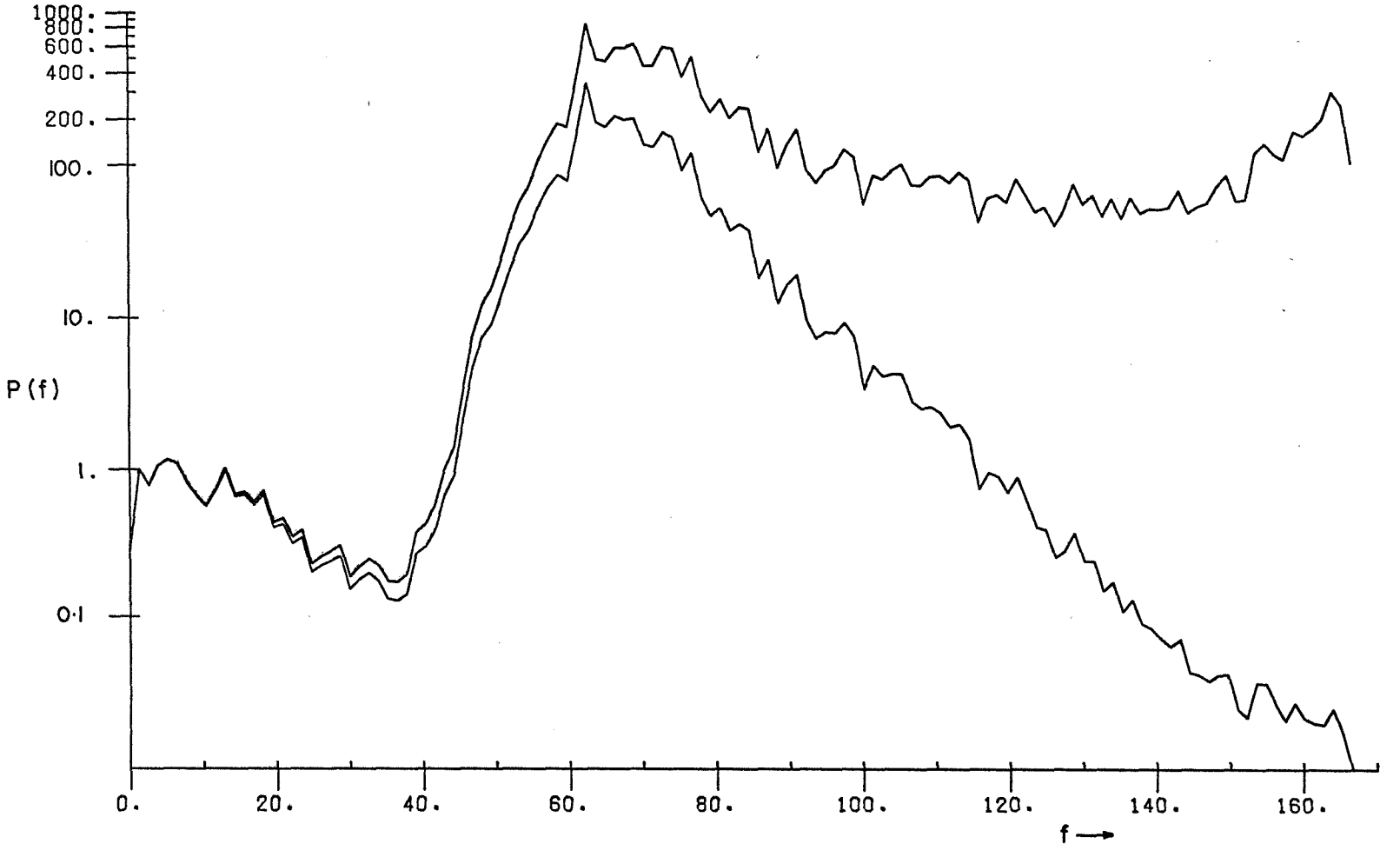

FIGURE 3B : POWER DENSITY SPECTRUM OF RECORD 13.

THE LOWER GRAPH IS THE SPECTRUM OF MEASURED SEA-BED PRESSURES.

THE UPPER GRAPH IS THE SPECTRUM CORRECTED FOR DEPTH ATTENUATION.

P(f) IN $MBAR^2/mHz$. f in mHz.

FIGURE 3C : POWER DENSITY SPECTRUM OF RECORD 19.

THE LOWER GRAPH IS THE SPECTRUM OF MEASURED SEA-BED PRESSURES.

THE UPPER GRAPH IS THE SPECTRUM CORRECTED FOR DEPTH ATTENUATION.

P(f) in $MBAR^2/mHz$. f in mHz.

FIGURE 3D : POWER DENSITY SPECTRUM OF RECORD 24.

THE LOWER GRAPH IS THE SPECTRUM OF MEASURED SEA-BED PRESSURES.

THE UPPER GRAPH IS THE SPECTRUM CORRECTED FOR DEPTH ATTENUATION.

P(f) in $MBAR^2/mHz$. f in Mhz.

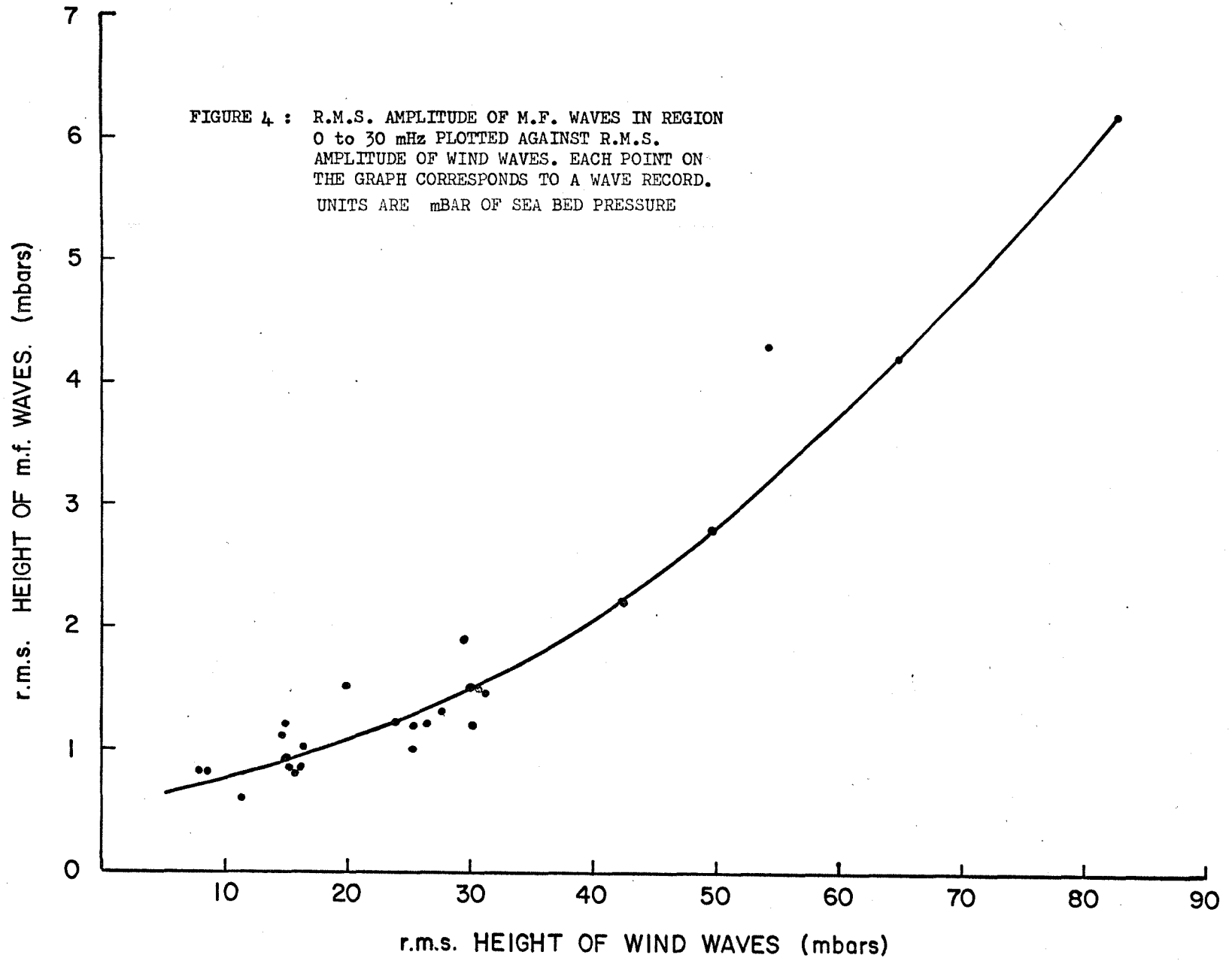

FIGURE 4 : R.M.S. AMPLITUDE OF M.F. WAVES IN REGION 0 to 30 mHz PLOTTED AGAINST R.M.S. AMPLITUDE OF WIND WAVES. EACH POINT ON THE GRAPH CORRESPONDS TO A WAVE RECORD. UNITS ARE mBAR OF SEA BED PRESSURE

FIGURE 5 : $\phi(\tau)$ - CROSS CORRELATION FUNCTION BETWEEN M.F. WAVES AND WIND WAVE ENVELOPE. WIND WAVE ENVELOPE IS MEAN SQUARE OF WIND WAVES OVER $2T_z$.

POSITIVE LAGS CORRESPOND TO WIND WAVES PRECEDING M.F. WAVES. LAG IN SECONDS.

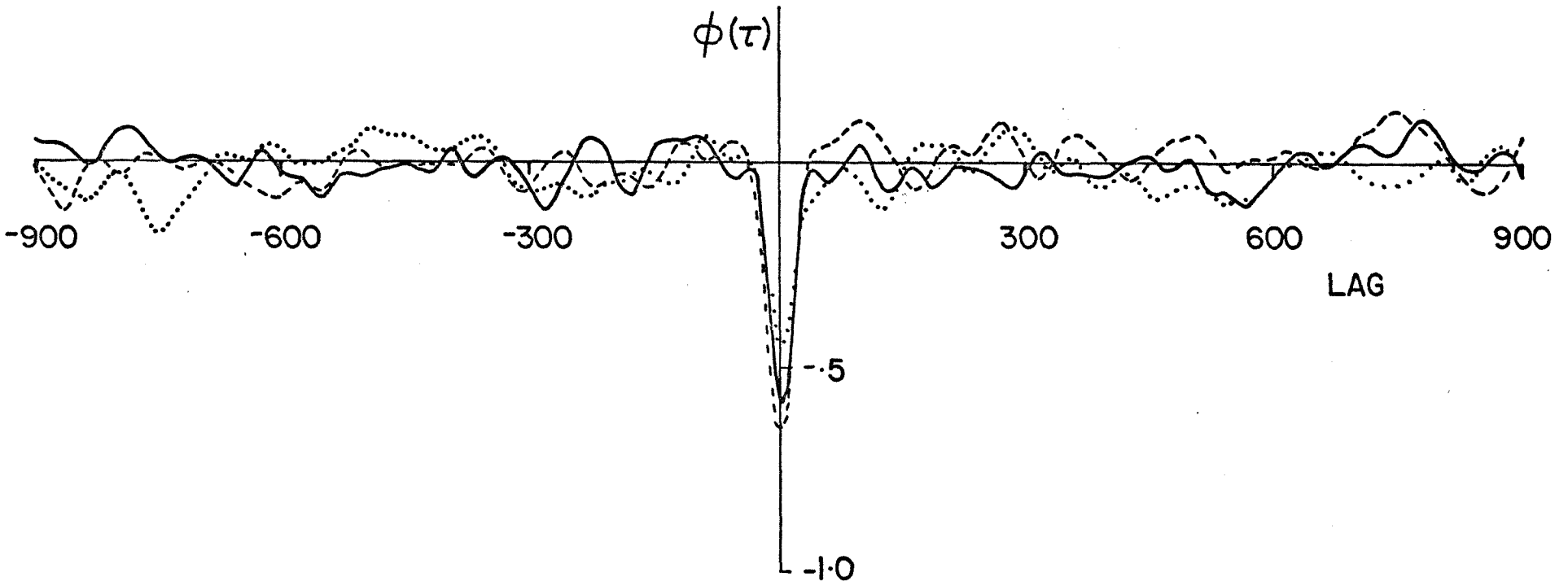

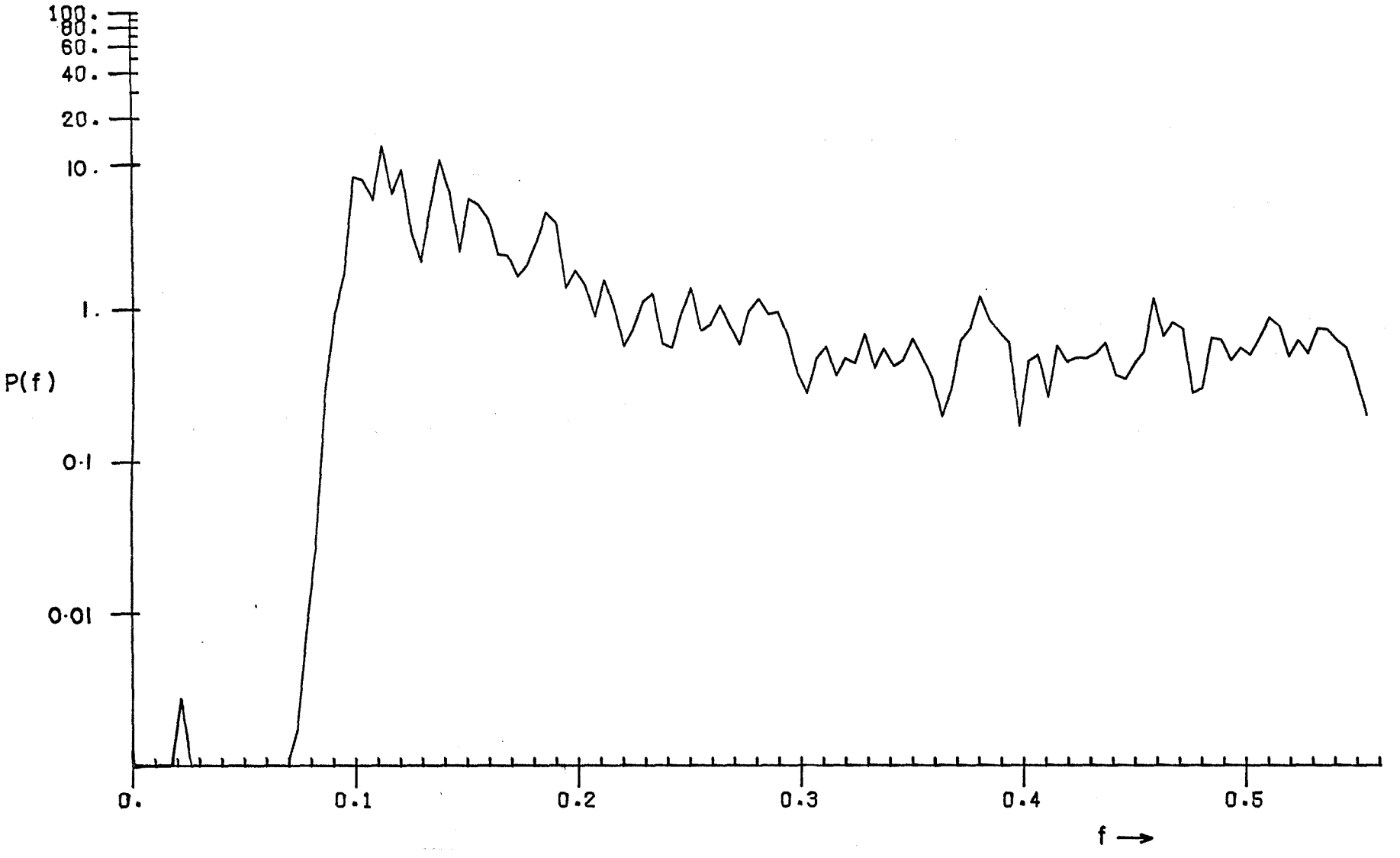

FIGURE 6 : SPECTRUM OF HIGH FREQUENCY TIDAL SERIES.
THE TIDES ARE REMOVED BY A COSINE TAPERED
FOURIER SERIES.

P(f) in mBAR /mHz f in mHz

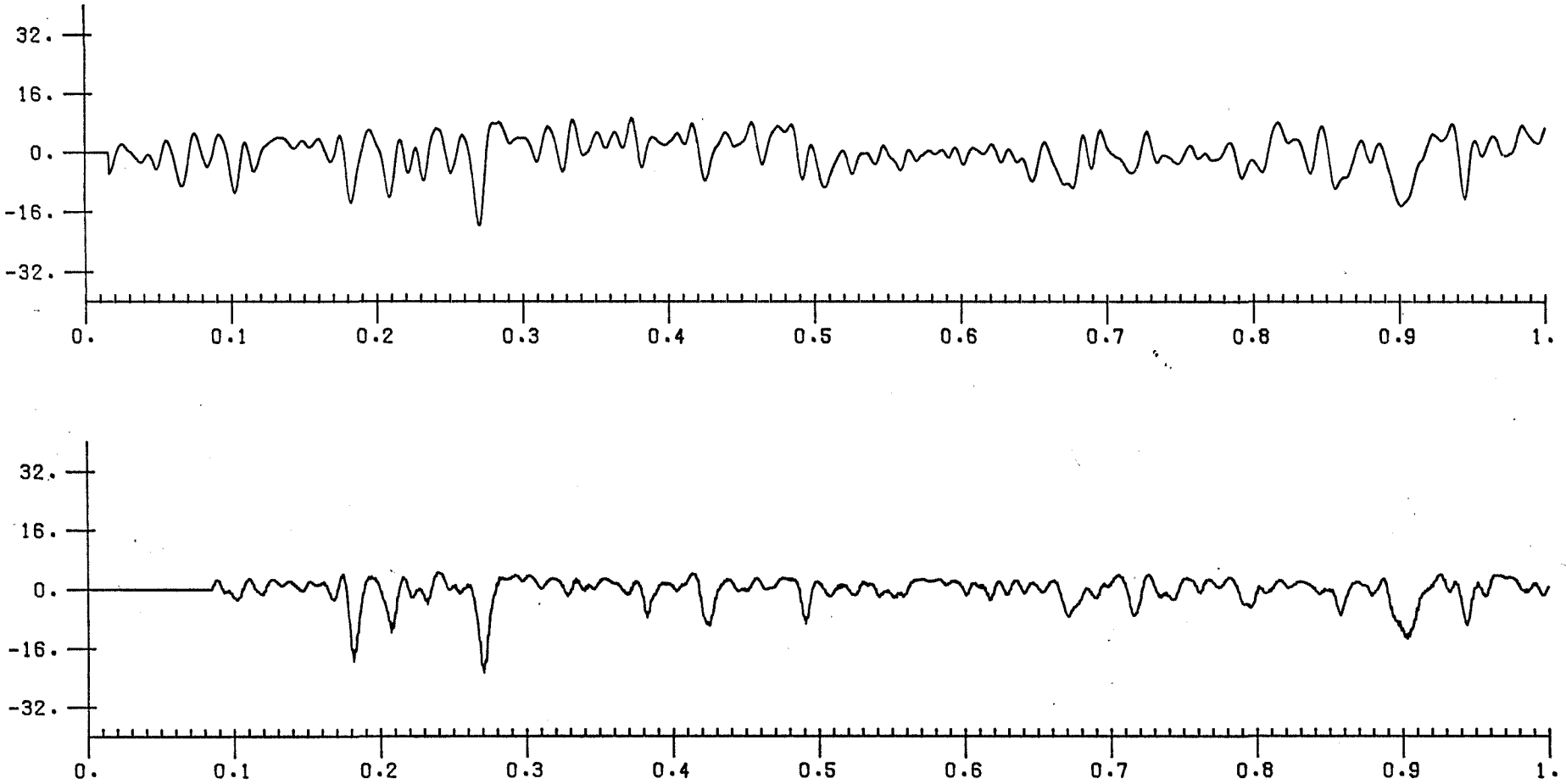

FIGURE 7: 1 HOUR OF M.F. PRESSURES FROM RECORD 13.
UPPER OBSERVED DATA.
LOWER PREDICTIONS FROM RESPONSE WEIGHTS.
UNITS mBAR.